

# NUMERICAL SIMULATION OF TENSILE LOADED LAP RIVETED JOINT

Elżbieta Szymczyk, Agnieszka Derewońko, Andrzej Kiczko

*Military University of Technology  
Faculty of Mechanical Engineering  
Department of General Mechanics  
2 Kaliskiego Street, 00-908 Warsaw, Poland  
tel.: +48 022 683 90 39; fax: +48 022 683 94 61;  
e-mail: e.szymczyk@wme.wat.edu.pl, a.derewonko@wme.wat.edu.pl*

**Jerzy Jachimowicz**

*Institute of Aeronautics  
Al. Krakowska 110/114, 02-256 Warsaw, Poland  
e-mail: jjachomowicz@ilot.edu.pl*

## **Abstract**

*The paper deals with the analysis of the global shell–beam model of a riveted lap joint consisting of six rivets. This is a stage of study of the local physical phenomena in riveted joint [3 – 12]. The contact with friction is defined between collaborating parts of the joint. The calculations are carried out in an elastic-plastic range. The influence of the specimen geometry, boundary conditions, rivet stiffness and the sheet material model on strain and stress fields in the riveted joint is studied. Numerical models are verified on the base of experimental tests.*

*In particular plastic strain fields during tensile loading, stress fields during tensile loading, comparison of numerical results, plastic strain fields around the hole, stress fields in the whole specimen are presented in the paper. Results demonstrated that the specimen geometry has important influence on the stress and strain fields in the final stage of tensile loading. The advantage of the numerical simulation is limiting development costs and improving analysis by giving more complete information about stress and strain fields compared to the pure experimental way. The stress and strain fields can be presented in the neighbourhood of a contact interface, where it is impossible to detect and measure it experimentally.*

**Keywords:** riveted joint, FEM, global model, nonlinear analysis

## **1. Introduction**

Riveting, particularly in aviation, is traditional but still commonly used joining method for metal and composite elements. Aircraft structures, like airplane or helicopter fuselages, wings etc. are thin-walled structures, with coverings made of thin sheets stiffened by stringers, frames or ribs. Sheets are typically assembled by multiple rivet or bolt joints. Rivets and bolts are used to joint sheets and stiffeners, as well.

Therefore fatigue resistance of the aircraft structure is depended on tens of thousands or even hundred of thousands rivet joints, which are used to build it [1, 2 and 4].

Thin-walled constructions are made of metal sheets or composite covers. Aluminium or titanium alloys are commonly used in aviation. In the paper aluminium alloy D16 (equivalent to 2024T4 or PA7T) is considered.

The paper presents a stage of study of the local physical phenomena in riveted joint [3 – 12]. Analysis of riveted structures requires a local–global approach in modelling.

The residual stress and strain state appears in the joint after the riveting process. Simulation of upsetting process is investigated using a local model [3, 5, 6 and 9]. Furthermore in service condition aircraft structures are subjected to variable cyclic loads [1, 2, 8 and 10].

The riveted joints are critical areas of the aircraft structure due to severe stress concentrations, plastic strain and effects such as surface damage (fretting wear) and secondary bending. Therefore the fatigue crack initiation starts at the rivet holes [1, 3 and 4]. Fretting fatigue is recognised as a surface damage phenomenon and describes situation where microslip between contacting surfaces appears to give rise to reduction in fatigue life [13]. Fretting depends on following reasons [4]: surface smoothness, hardness of mating elements, magnitude of normal and tangential forces and relative displacement amplitude and frequency. Mechanical conditions causing initiation of fretting phenomena is analysed using local models [5 – 10]. Influence of the residual stresses and tensile loading on relative displacement and contact forces between the rivet and the hole is presented in the paper [8]

The global models allow to analyse selected parts of structure and provide the necessary data to define boundary conditions for the local models [10].

Global numerical models are developed to analyse strain and stress fields around the rivet holes during tensile loading and to determine the load carrying ability of the joint. The global model of six rivet specimen is considered in the paper. The numerical FEM calculations of three-dimensional beam–surface model are performed with the NASTRAN code [14].

## **2. Models of riveted specimens**

The calculations are carried out for various shapes of the lap riveted joint. The shape of basic specimen (specimen 1) is presented in figure 1. The sample consists of two aluminium sheets (50 mm wide and 157 mm long) connected by six steel rivets. The numerical models describe symmetric part of the joint. Thickness of the upper sheet is equal 2.9 mm, otherwise thickness of the lower one changes from 2.5 mm to 3.7 mm (fig 1). There are a number of ways in which a riveted joint may fail. Local change of the lower sheet thickness ensures predictable and repetitive failure behaviour. The crack initiation starts at a hole located in the left hand side rivet row of the upper sheet and fracture occurs between the rivets of this row (fig. 2).

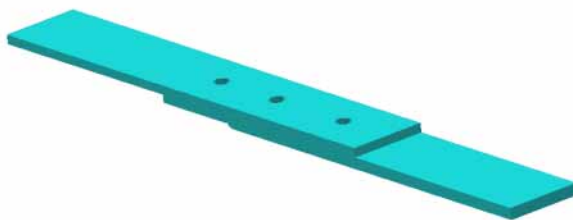


*Fig. 1. Basic specimen geometry*



*Fig. 2. Specimen after tensile loading*

The calculations are carried out for several cases of sheet geometry and some ways of fixing in the grips of testing machine. The clamping surface of the grips is 35 mm wide. Therefore gripping tabs of the specimen should be narrowed from 50 mm to maximum 35 mm. Specimen 2 describes sheets with gripping tabs 35 mm wide and 50 mm long (fig 3a). Whereas specimen 3 has gripping tabs 25 mm long (fig 3b). Specimen 4 is made by cutting the basic specimen in two parts 25 mm wide.

Boundary conditions taking into consideration are shown in figure 4.

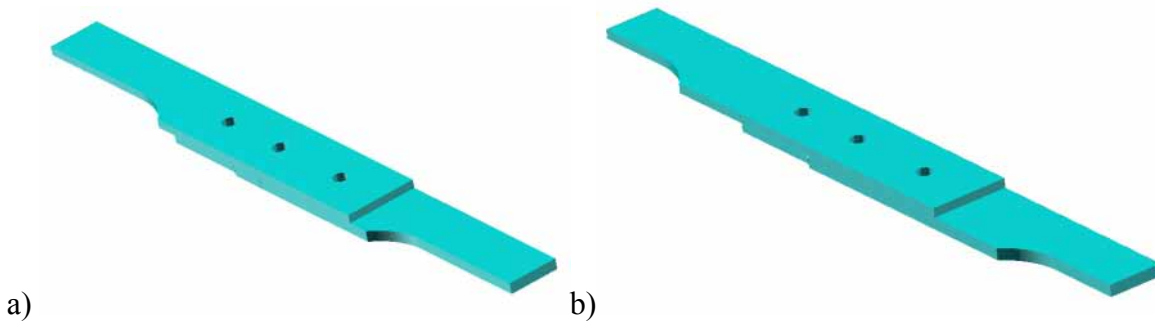


Fig. 3. Specimen geometry a) specimen 2, b) specimen 3

	a	b
specimen 1		
specimen 2		
specimen 3		

– gripping tabs

Fig. 4. Boundary conditions for all specimens

However grips of the testing machine are positioned vertically (in one plane) one above the other. The relative shift of the middle surfaces of upper and lower sheets equals 3.3 mm. Therefore initial displacement of the gripping tabs of the upper sheet is considered. Two steps of the specimen loading are presented in fig. 5.

The influence of the rivet stiffness on stress and strain fields and tearing load level is investigated. The rivet is modelled as rigid element or as beam element (5 mm cross section diameter).

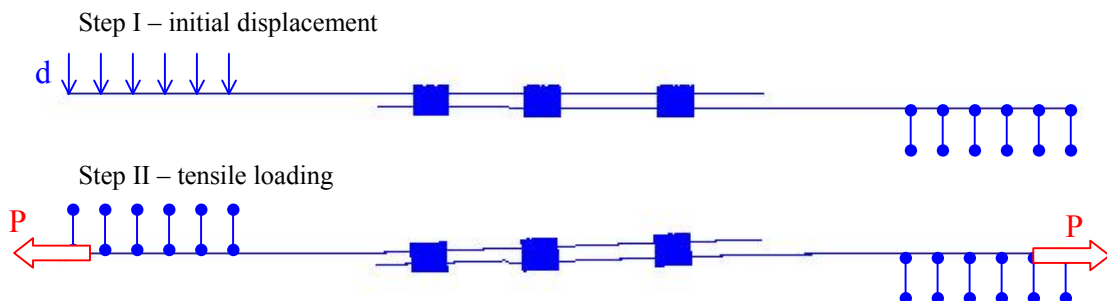


Fig. 5. Two step loading

Two material models of D16 aluminium alloy are taken into consideration. Bilinear and trilinear stress-strain curves, describing model a) and model b) respectively, are shown in fig. 6.

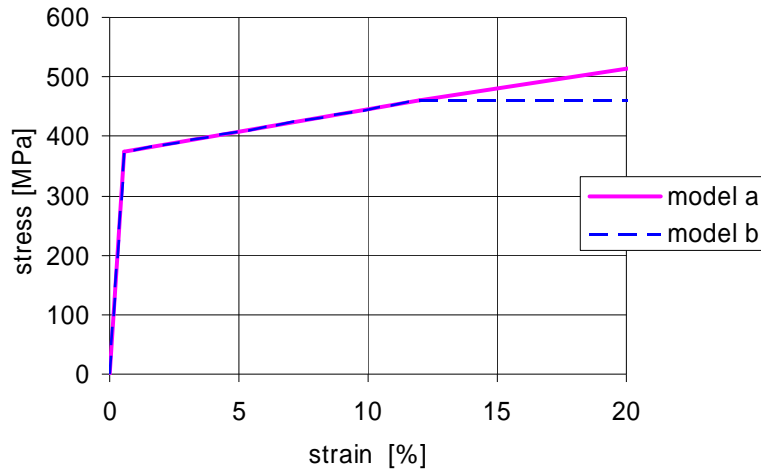


Fig. 6. Stress- strain curves

The finite element models are built with Patran. Nastran code is used to perform nonlinear analysis.

#### 4. Results

Numerical calculations are performed to estimate tearing (ultimate) force and observe the mechanism of the specimen failure. Finite element stress and strain analysis is performed to determine plastic fields in the sheets and load magnitude corresponding to initiation of plastic deformations around a rivet hole. Numerical results are in satisfactory agreement with analytical predictions and experimental tests.

The plastic strain fields in the basic specimen (specimen 1) during tensile loading are shown in fig 7. The same results for specimens 2, 3 and 4 are shown in fig. 8, 9 and 10 respectively. Full plasticity of the upper sheet cross section (specimen 1 and 4) occurs in the left hand side rivet row (fig 7). Specimens 2 and 3 have tendency to break (yield) in the grips (fig 8 and 9). Von Misses stress fields during tensile loading for the basic specimen are shown in fig 11.

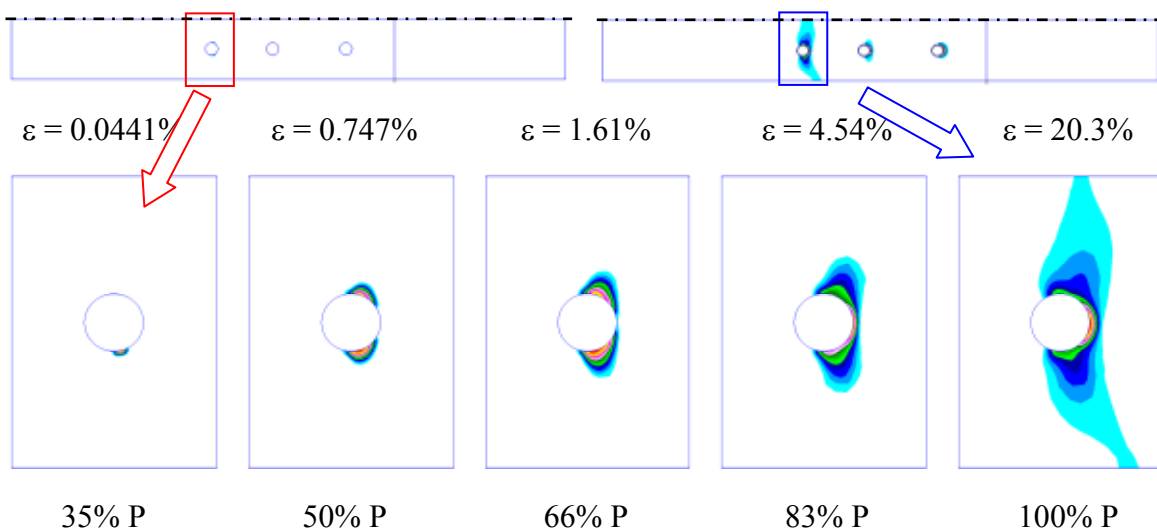


Fig. 7. Plastic strain fields during tensile loading – specimen 1

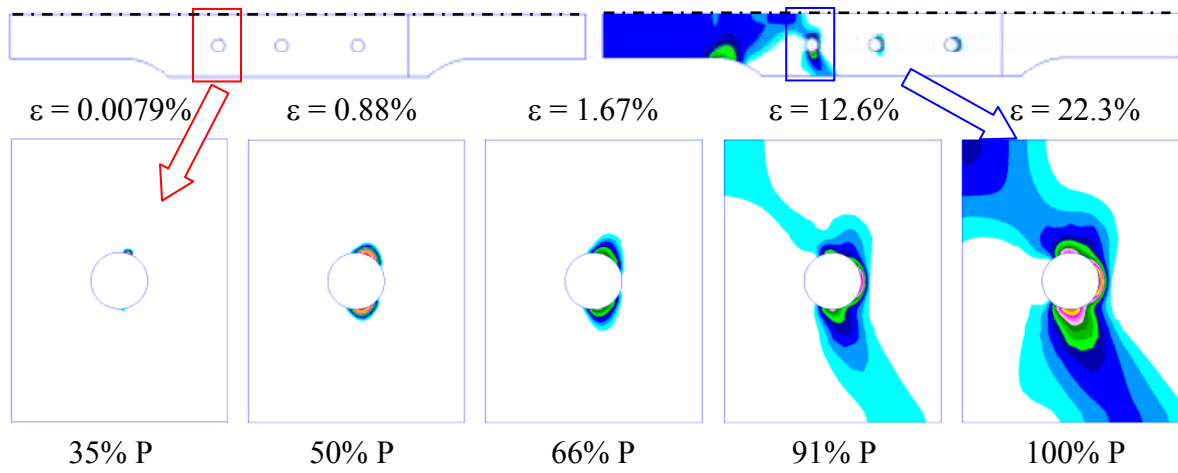


Fig. 8. Strain fields during tensile loading – specimen 2

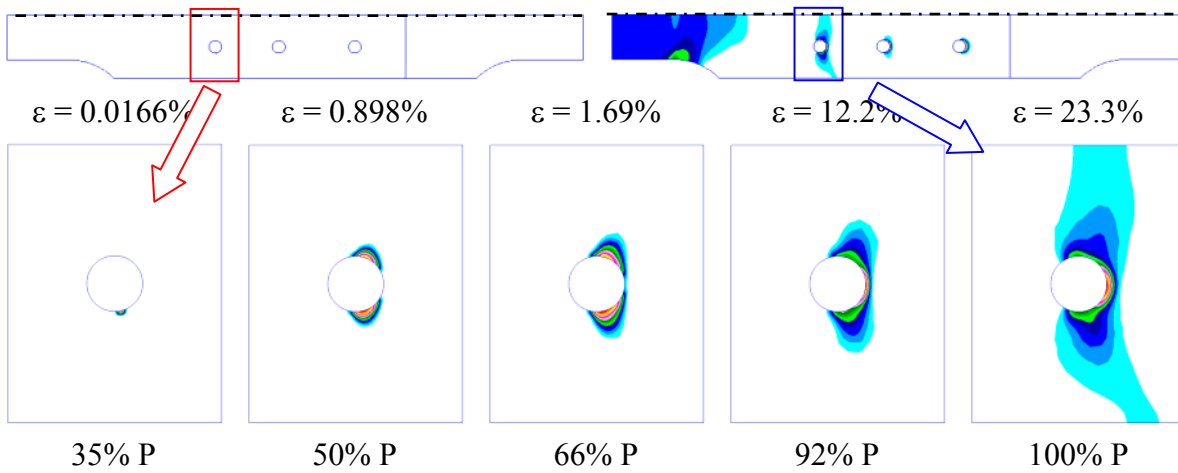


Fig. 9. Strain fields during tensile loading – specimen 3

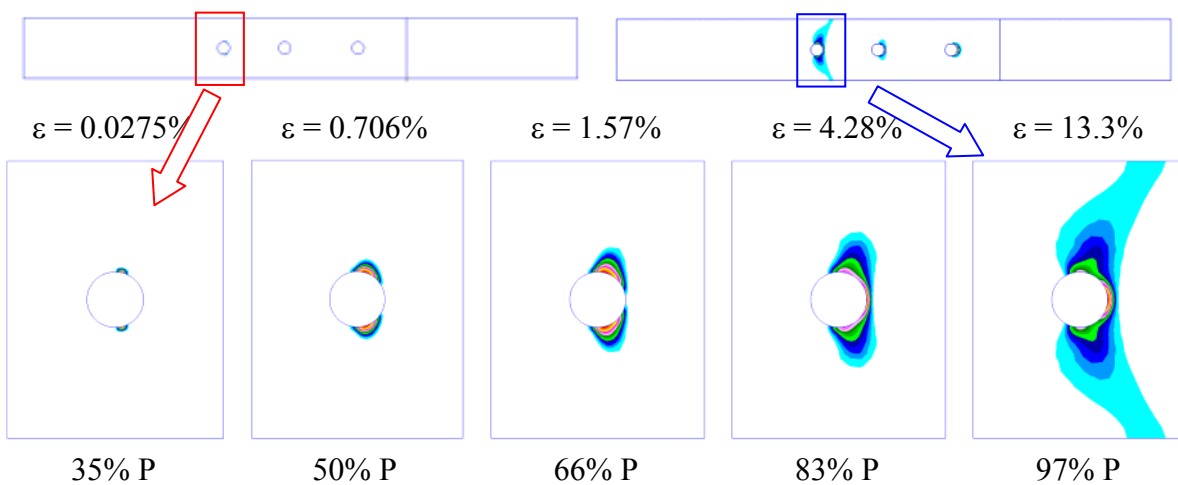


Fig. 10. Strain fields during tensile loading – specimen 4

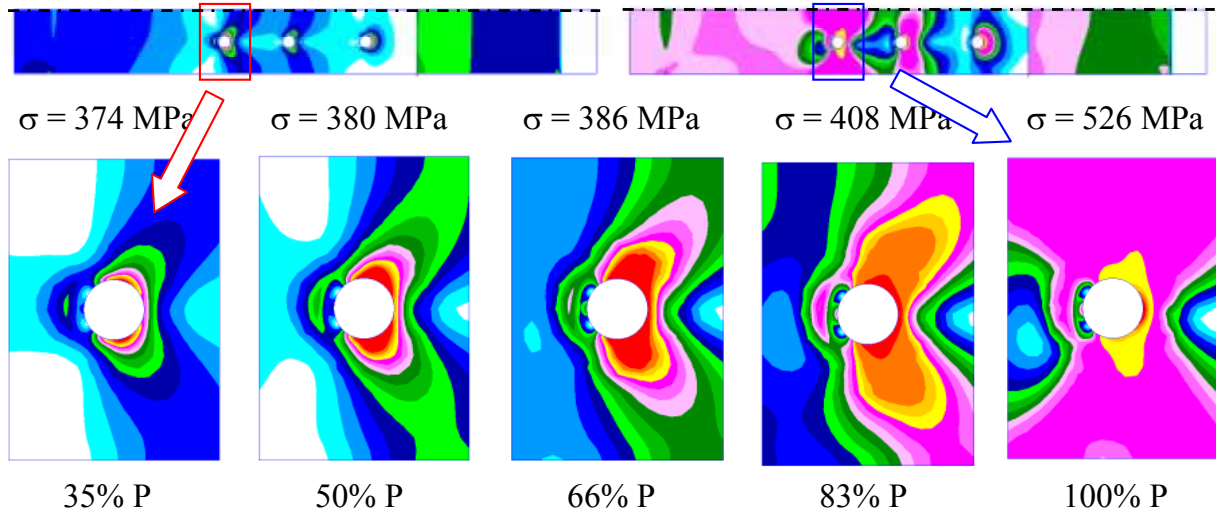


Fig. 11. Stress fields during tensile loading – specimen 1

In the numerical calculation tearing force is recognised as a load causing full plasticity of the specimen cross section. The ultimate load is equal 45 kN for the basic specimen.

The numerical results ( $F_p$  – load level corresponding to initiation of plastic deformation around the rivet hole,  $F_n$  – breaking load,  $\epsilon_{max}$  – maximum plastic strain,  $\sigma_{max}$  – maximum equivalent stress) for various specimen geometry and different boundary conditions are presented in table 1.

Tab. 1. Comparison of numerical results

boundary conditions	geometry		specimen 1	specimen 2	specimen 3
a	$F_p$	[kN]	15.7	15.4	15.4
	$F_n$	[kN]	45	41.8	41.8/45
	$\epsilon_{max}$	[%]	21.6	12.6	12.2/23.3
	$\sigma_{max}$	[MPa]	536	468	466/549
b	$F_p$	[kN]	15.7	15.4	15.4
	$F_n$	[kN]	45	41.8	37.2/45
	$\epsilon_{max}$	[%]	21.5	12.6	4.27/23.4
	$\sigma_{max}$	[MPa]	535	466	406/549

Maximum load recorded in experimental test, before specimen rupture, equals 39.6 kN. The numerical predictions are about 14% higher ( $P = 45$  kN).

Both material models are equivalent for strain below 10%. The rivet stiffness has no influence on the moment of initiation of plastic deformation at a rivet hole. The differences in strain (fig 12) and stress (fig 13 and 14) distributions occur in the final stage of tensile loading. The specimen tearing load is equal 43 kN (96% P).

Maximum value of the plastic strains for material model b is two times greater than for model a.

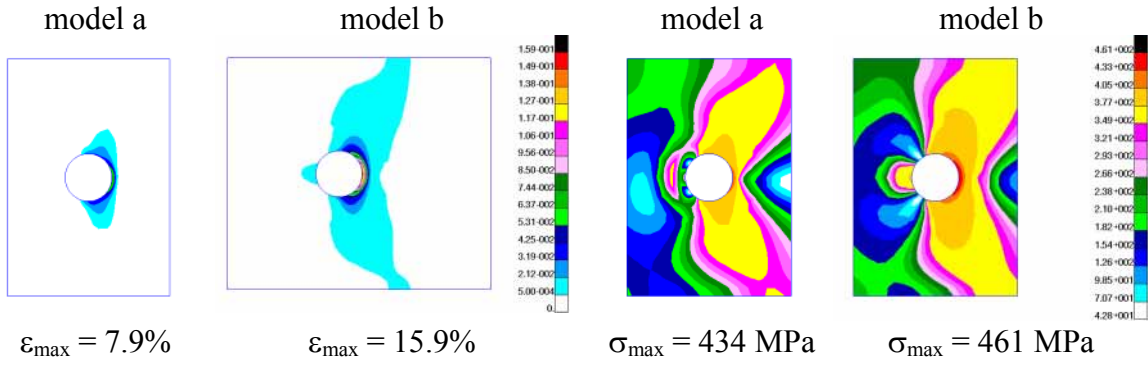


Fig. 12. Plastic strain fields around the hole

Fig. 13. Stress fields around the hole

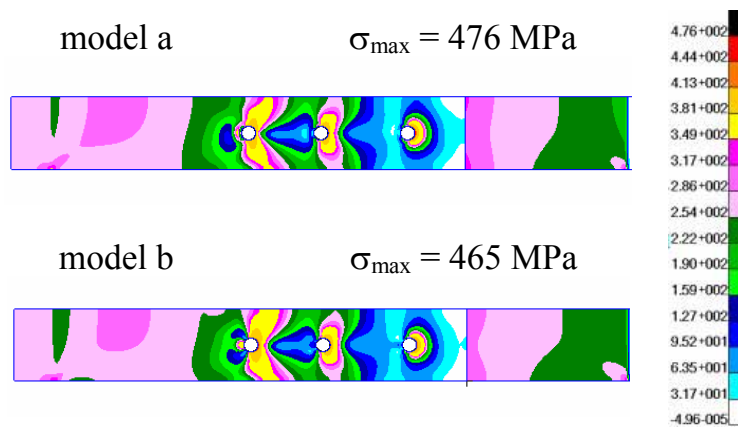


Fig. 12. Stress fields in the whole specimen

## 5. Conclusions

Analysis of the global model of the tensile loaded riveted joint is performed. The objective of the paper is to determine loads causing initiation of plastic deformations at a rivet hole and failure of the specimen by sheet tearing between rivet holes.

The specimen geometry has important influence on the stress and strain fields in the final stage of tensile loading. The failure mode of specimen 1 is upper sheet tearing in the left hand side rivet row, whereas specimens 2 and 3 tend to break (yield) in the grips of testing machine.

The first stage of plastic deformations around a rivet hole, for load level 35% to 50% of ultimate load, is similar for all specimen geometry and boundary conditions.

The boundary conditions (clamping surface of the grips) have no influence on the level of ultimate load (tab 1).

The developed and validated models can be used in the analysis of specimen behaviour during cyclic loading.

The advantage of the numerical simulation is limiting development costs and improving analysis by giving more complete information about stress and strain fields compared to the pure experimental way

The deformations obtained in the global analysis determine the boundary conditions in a local model where simulation of the riveting process can be performed [10]. The stress and strain fields can be presented in the neighbourhood of a contact interface, where it is impossible to detect and measure it experimentally.

## Acknowledgements

This work was carried out with the financial support of Polish Scientific Research Committee (KBN) under research grant No 0 T00B 007 25.

## References

- [1] Muller, R., *An experimental and numerical investigation on the fatigue behaviour of fuselage riveted lap joints*, Doctoral Dissertation, Delft University of Technology, 1995.
- [2] Langrand, B., et al., *An alternative numerical approach for full scale characterisation for riveted joint design*. *Aerospace Science and Technology* 6, 343–354, 2002.
- [3] Ciesielski, M., Jachimowicz, J., Kajka, R., J. Krysztofik, J., Szachnowski, W., *Analytical and experimental stress field image in a rivet joint*, *Transaction of the Institute of Aviation*, Warsaw, 1, 14–19, 2005.
- [4] Jachimowicz, J., Kajka, R., Kaniowski, J., Karliński, W. *Fretting in the aircraft structures*, *Tribologia, SIMPRESS Warszawa*, 3, 97–108, 2005 (in polish).
- [5] Niezgodzinski, T., Młotkowski, A., *Das numerische Modellieren der Nietung*, GESA Symposjum, Saarbrucken 2005.
- [6] Derewońko, A., Szymczyk, E., Jachimowicz, J., *Numeryczna symulacja procesu nitowania*, IX Konferencja Naukowo-Techniczna Programy MES w Komputerowym Wspomaganiu Analizy Projektowania i Wytwarzania Giżycko, 19÷22 10 2005
- [7] Jachimowicz, J., Kajka, R., Krysztofik, J., Szachnowski, W., Szymczyk E., *Stan odkształceń i naprężeń w pobliżu nitu w konstrukcji lotniczej – analizy mes i badania*, IX Konferencja Naukowo-Techniczna „Programy MES w Komputerowym Wspomaganiu Analizy Projektowania i Wytwarzania” Giżycko, 19÷22 10 2005
- [8] E. Szymczyk, E., Jachimowicz, J., Derewońko, A., *Analysis of displacement and stress distributions in riveted joint*, III European Conference on Computational Mechanics Solids, Structures and Coupled Problems in Engineering, Lisbon, Portugal, 5–8 June 2006
- [9] Derewońko, A., E. Szymczyk, E., Jachimowicz, J., *Numerical simulation of riveting process*, 6th European Solid Mechanics Conference ESMC, Budapest, Hungary, 28 August – 1 September, 2006
- [10] Derewońko, A., Szymczyk, E., Jachimowicz, J., *Analiza połączenia nitowego z uwzględnieniem naprężeń resztkowych i eksploatacyjnych*, Polanica 21-24.06 2006
- [11] Jachimowicz, J., Kajka, R., Szachnowski, W., Szymczyk E., *Problemy eksploatacji szwów nitowych w konstrukcjach lotniczych – analityczna i eksperymentalna ocena stanu naprężeń*, Polanica 21-24.06 2006
- [12] Jachimowicz, J., *Założenia do badań i pomiarów połączeń nitowych*, Opracowanie wewnętrzne ZMO, 11. 2003
- [13] Nowell, D., Recent developments in the understanding of fretting fatigue. *Engineering Fracture Mechanics* 73, 207-222, 2006.
- [14] *MSC Nastran Theoretical Manual*, MSC Corp. 2004